

AOARD REPORT

Contract No. 084003

Slurry Spray and Sintering Method for Fabricating FGM (Functionally Graded Material) Thermal Barrier Coatings

Sook-Ying Ho, Andrei Kotousov, Phuc Nguyen

School of Mechanical Engineering
The University of Adelaide
Adelaide, SA 5000
AUSTRALIA

28 February 2008

AOARD Program Manager: Dr. Kumar Jata

Report Documentation Page			Form Approved OMB No. 0704-0188		
Public reporting burden for the collection of information is estimated to average 1 hour per response, including the time for reviewing instructions, searching existing data sources, gathering and maintaining the data needed, and completing and reviewing the collection of information. Send comments regarding this burden estimate or any other aspect of this collection of information, including suggestions for reducing this burden, to Washington Headquarters Services, Directorate for Information Operations and Reports, 1215 Jefferson Davis Highway, Suite 1204, Arlington VA 22202-4302. Respondents should be aware that notwithstanding any other provision of law, no person shall be subject to a penalty for failing to comply with a collection of information if it does not display a currently valid OMB control number.					
1. REPORT DATE 20 JUL 2009		2. REPORT TYPE Final		3. DATES COVERED 14-02-2008 to 14-03-2009	
4. TITLE AND SUBTITLE Functionally Graded Material Thermal Barrier Coatings for Hypersonic Structures Design and Thermal Structural Analysis				5a. CONTRACT NUMBER FA48690814003	
				5b. GRANT NUMBER	
				5c. PROGRAM ELEMENT NUMBER	
6. AUTHOR(S) Sook Ying Ho				5d. PROJECT NUMBER	
				5e. TASK NUMBER	
				5f. WORK UNIT NUMBER	
7. PERFORMING ORGANIZATION NAME(S) AND ADDRESS(ES) University of Adelaide,Adelaide,Adelaide SA 5005,Australia,NA,NA				8. PERFORMING ORGANIZATION REPORT NUMBER N/A	
9. SPONSORING/MONITORING AGENCY NAME(S) AND ADDRESS(ES) AOARD, UNIT 45002, APO, AP, 96337-5002				10. SPONSOR/MONITOR'S ACRONYM(S) AOARD	
				11. SPONSOR/MONITOR'S REPORT NUMBER(S) AOARD-084003	
12. DISTRIBUTION/AVAILABILITY STATEMENT Approved for public release; distribution unlimited					
13. SUPPLEMENTARY NOTES					
14. ABSTRACT In this study functionally gradient metal-ceramic coatings were fabricated using low cost slurry and sintering process. The quality of FGM coatings was evaluated through microstructure analysis, thermal cycling tests (60 minutes at 900C followed by 30 minutes cooling), and post fracture analysis.					
15. SUBJECT TERMS					
16. SECURITY CLASSIFICATION OF:			17. LIMITATION OF ABSTRACT Same as Report (SAR)	18. NUMBER OF PAGES 35	19a. NAME OF RESPONSIBLE PERSON
a. REPORT unclassified	b. ABSTRACT unclassified	c. THIS PAGE unclassified			

Table of Contents

1.	Introduction	3
2.	Optimisation of the Wet Powder (Slurry) Spray and Sintering Method for Fabricating FGM Thermal Barrier Coatings	
2.1	TBCs specimen preparation	7
2.2	Optimisation of FGM coating	10
3.	Results and Verification	
3.1	Microstructural Analysis	13
3.2	Thermal and Mechanical Testing	
3.2.1	Thermal Cycling	22
3.2.2	Adhesion Test	26
4.	Summary and Future Plans	29
5.	Acknowledgements	31
6.	References	31

1. Introduction

Ceramic-metal functionally graded materials (FGMs) have been attracting a great deal of attention as thermal barrier coatings (TBCs) for aerospace structures working under super high temperatures and thermal gradients. FGM is a relatively new concept involving tailoring the internal microstructure of composite materials to specific applications, producing a microstructure with continuously varying thermal and mechanical properties at the continuum or bulk level. Hence, they are ideal for applications involving severe thermal gradients, such as the environments encountered by hypersonic flights because the microstructural grading of FGM TBCs could be adjusted to help reduce the mismatch in thermomechanical properties, which induce high thermal stresses in the structure.

This study is aimed at developing FGM thermal barrier coatings suitable for high-speed flight applications. Our earlier study^{7, 8} on aerothermal-structural analysis of hypersonic vehicles for flight tests identified design criteria (such as appropriate temperature limit) for designing FGM TBCs. Preliminary results from a previous study supported by AOARD under contract number 064043 suggested that FGM TBCs produced by the Slurry Spray and Sintering method exhibited sufficient durability to survive in hypersonic flight environments where the operational time is relatively short. The adhesion strength of coatings produced by this method is likely to be adequate for applications such as expendable hypersonic vehicles where the TBCs are not required to have long life expectancy. For such applications, the Slurry Spray and Sintering method offers considerable advantages in terms of cost effectiveness and relatively simple fabrication process. However, for applications where long life expectancy is required (for example, nuclear reactors) the more expensive techniques (such as chemical vapour deposition, plasma spraying, etc.) which produce TBCs with higher failure adhesion strength would be more appropriate.

The Wet Powder (Slurry) Spray and Sintering method reported in our previous study³² was relatively undeveloped and under utilised compared to more expensive techniques such as chemical vapour deposition, physical vapour deposition, plasma spraying and powder metallurgy. It utilised a pressurised spray gun to spray a slurry

mixture of the powdered coating material suspended in a liquid solution directly onto a substrate surface followed by sintering using an oxyacetylene torch.

The previous study (AOARD-064043) investigated the effects of slurry composition, type of ceramic powder, compatibility with substrates, spraying and sintering conditions. Several TBC specimens have been fabricated under various conditions to develop a procedure which produced good quality coatings (of up to 3 layers) with little or no spallation. The optimum time, heat flux and applied pressure level for sintering were deduced. TBCs produced from a 40-45% ceramic, 4% binder and 0.4% dispersant composition and sintered for 30 minutes with an applied pressure of 30 MPa produced good quality coatings with a uniform and very smooth surface. Scanning electron micrographs of the fabricated TBC coatings showed good contact between the grain boundaries of the ceramic powder.

This is a report on a follow-on study to AOARD-064043 to investigate the fabrication of advanced thermal barrier coating materials, such as ceramic-metal FGMs which have high heat resistance and low thermal stress properties under high temperature conditions. The study is conducted in conjunction with development of micromechanics models and aero-thermal-structural predictive tools, as part of a strategy to design advanced thermal barrier coatings for application to hypersonic vehicles.

In the present study, the (Wet Powder) Slurry and Sintering method is further developed to improve the quality of the FGM TBC and optimise the fabricating conditions. A more extensive microstructure analysis, thermal and mechanical testing program is conducted to 1) obtain a more quantitative measure of the quality and durability of the FGM thermal barrier coatings and 2) develop high temperature constitutive models for input into the finite element (FE) modelling to predict the thermal-structural response of structures with FGM thermal barrier coatings.

The theoretical component of the previous project³² studied the micromechanics modelling of multi-phase composites and finite element modelling of the aerothermal-structural response of hypersonic structures, with the view to predict the global thermal-structural response of FGM thermal barrier coated structures.

These micromechanics models¹⁻² and aero-thermal-structural analysis capability³ will provide the theoretical and analytical basis for our current study on design and optimisation of ceramic-metal FGM's and TBC coated structures. One aspect of our theoretical studies is the application of the mean-field micromechanical approach to design ceramic-metal FGM thermal barrier coatings. This analysis took into consideration the microscopic inelastic deformation in each constituent phase such as plastic and creep, as well as the diffusional mass flow at the interface between the ceramic and metal phases. A case study for Ni-ZrO₂ FGM TBCs was conducted to help develop a fundamental strategy for optimal design of ceramic-metal FGMs. Extensive experimental work is needed to validate the numerical results obtained in that study^{3, 32} and this will be conducted in Option 1 of the current project, if time permits.

The milestones of the current study are:

- *Improvement of the Wet Powder (Slurry) Spray and Sintering method for fabricating FGM's.* This includes optimising the fabrication conditions and designing an automated sintering platform to enable automation of the sintering process or sintering in an oven under controlled conditions, to produce high quality FGM coatings. Also, adapting the technique to spray and sinter the internal surfaces of cylindrical ducts, for applications such as combustors of air-breathing engines.
- *Microstructure and thermo-mechanical testing of the fabricated FGM TBCs.* The microstructure and integrity of the graded coatings on base metals will be studied using standard facilities available at the School of Mechanical Engineering and Adelaide Microscopy Centre at the University of Adelaide. High temperature mechanical properties of the FGM TBCs will be measured using the induction heating method developed in an earlier study³¹. Failure analysis will also be carried out with the view to adjusting the fabrication process and parameters to reduce interfacial spallation. The thermal and mechanical tests to be conducted include adhesion failure strength, micro-hardness indentation, thermal conductivity and tensile strength.
- *Thermal testing of FGM coated structures under realistic heating and pressure loading conditions.* A combustion test rig will be designed and hot

structures test techniques will be used to test the thermal-mechanical performance of structures coated with FGMs (Option 1).

- *Micromechanics modelling of multi-phase composites.* The theoretical studies of transformation toughening and constitutive equations of multi-phase composites will continue. Constitutive equations of multi-phase composites at elevated temperatures will be formulated to take into account stress concentration, thermal expansion, creep deformation of each phase, plastic deformation in the metal phase, and mass transfer at the interface between the ceramic and metal phases (Option 1).
- *Finite element method modelling of thermal-structural response of FGM coated structures.* The aero-thermal-structural analysis capability developed in our earlier studies will be used in this project to assist the design of FGM thermal barrier coatings at the material and global levels. At the material level, the micromechanics models will be implemented in finite element models of the FGM coatings, to determine the number of graded coating layers required to protect the metal structure (substrate) from the aerodynamic and combustion heating loads expected in hypersonic flights (Option 1).

2. Optimisation of the Wet Powder (Slurry) Spray and Sintering Method for Fabricating FGM Thermal Barrier Coatings

2.1 TBCs specimen preparation

The fabrication process in the Slurry Spray and Sintering method developed in our earlier study was described in detail in reference 32 and is summarized in the Figure below.

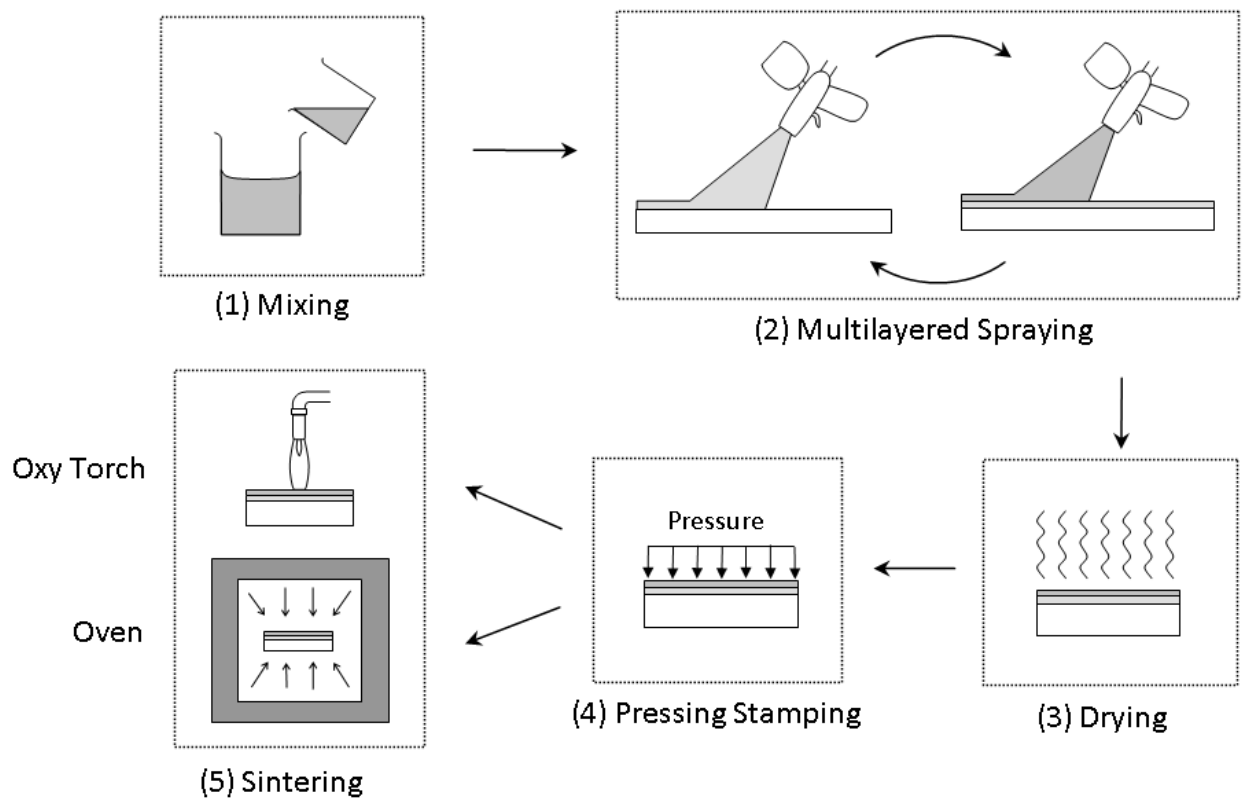


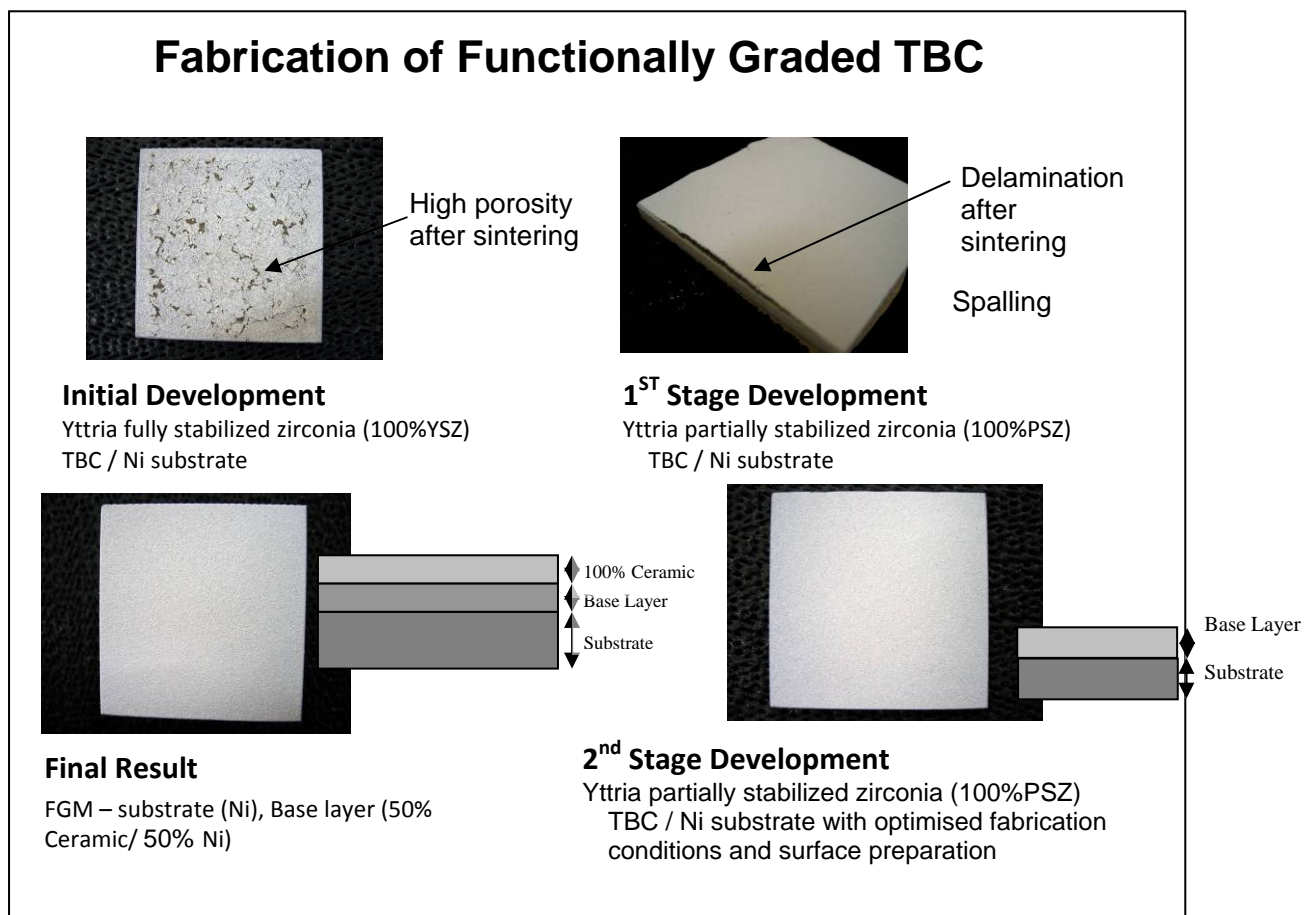
Figure 1: Slurry Spray and Sintering Method

The fabrication process consists of the following steps:

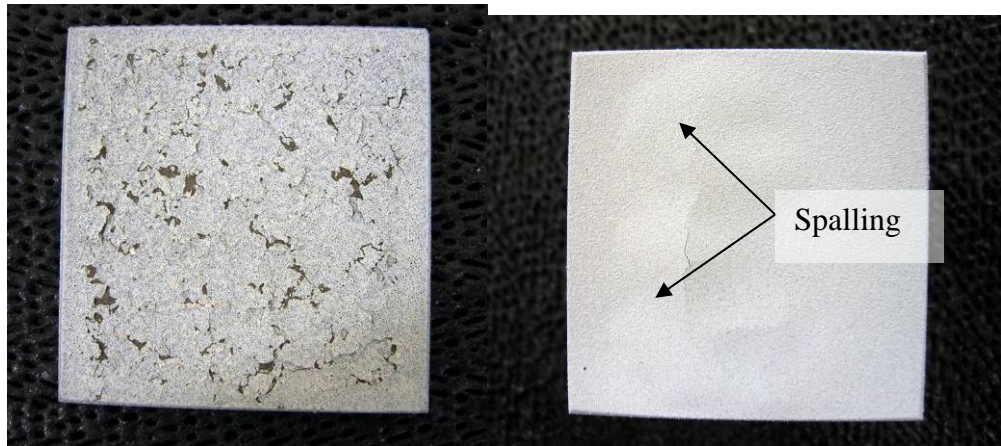
1. **Mixing**: the slurry is prepared from a mixture of ceramic and metal compounds, binder, dispersant and distilled water.

2. **Spraying:** the slurry mixture is then sprayed onto the substrate to form a wet coating. Spraying is effected using a normal gravity fed spray gun.
3. **Drying:** The coated substrates is left to dry at ambient conditions. Steps 2 and 3 are repeated for each subsequent layer to produce a functionally graded coating.
4. **Pressing Stamping:** The dried coating(s) are then pressure stamped to compact the layers.
5. **Sintering:** The Substrate is sintered using an automated sintering rig with oxy-acetylene torch or using a laboratory oven.

The stages in the development of the functionally graded TBC are summarized below:



In the initial development, yttria fully stabilized zirconia (YSZ) was compared with yttria partially stabilized zirconia (PSZ) as the base ceramic powder. No differences between the YSZ and PSZ powder were observed during the mixing process. However, the coating produced from YSZ powder showed high porosity and poor adhesion strength after sintering. This caused the TBC to spall during the cooling phase. The coating produced from PSZ showed improved bonding and adhesion strength after sintering, however high porosity still existed, causing some spalling (see Figure below).



Spalling of YSZ TBC after sintering

Spalling of PSZ TBC after sintering

In the first stage development, steps were taken to improve the adhesion strength between the TBC and the substrate to prevent delamination. These included surface preparation by sandblasting and cleaning the surface of the substrate with solvent prior to coating, and base layer improvement.

In the second stage development, the base layer was improved by varying the zirconia and nickel composition ranging from 25% to 50% and determining the best base layer adhesion strength. This single layer coating however, exhibited a high thermal conductivity due to the presence of nickel in the base layer coating.

Finally, a functionally graded coating consisting of a 50/50 ceramic/nickel base layer coating and a 100% ceramic coating top layer was fabricated. Low thermal

conductivity was achieved as a result of the introduction of a pure ceramic surface coating on top of the base layer.

2.2 Optimisation of FGM Coating

Optimisation of the quality and durability of the FGM thermal barrier coatings was achieved by systematically varying the parameters and conditions in the fabrication process. The optimum parameters and conditions for each fabrication process are described below.

The Table below summarizes the optimum composition of the slurry mixture for the base layer (comprising 50% pure nickel powder and 50% yttria partially stabilized zirconia, PSZ) and the top layer (100% PSZ). The binder is polyvinyl alcohol (PVA) and dispersant is tetra sodium pyrophosphate as described in detail in our previous report³².

		100 ml	200 ml	300 ml
100% PSZ	PSZ	45	90	135
	Nickel	0	0	0
50% PSZ 50% Ni	PSZ	22.5	59.4	89.1
	Nickel	22.5	30.6	45.9
Binder		3	6	9
Dispersant		0.4	0.8	1.2
Distilled water		51.6	102.2	153.8

Table 1: Optimum slurry mixture composition

Slurry Composition

It was found that the viscosity of the slurry mixture directly affects the quality of the thermal barrier coating sprayed onto the surface, as it directly affects the size of the spray droplets. The viscosity of the slurry mixture decreases with the amount of binder added (see Figure 2a). The optimum amount of binder was found to be 3%. It was also noted that the viscosity decreases proportionally with ceramic content in the

slurry mixture. Hence the percentage of the binder content of the slurry mixture for each functionally graded (FG) layer of the TBC should be adjusted to maintain the optimum viscosity of 25 centistokes, to minimise porosity induction during spraying.

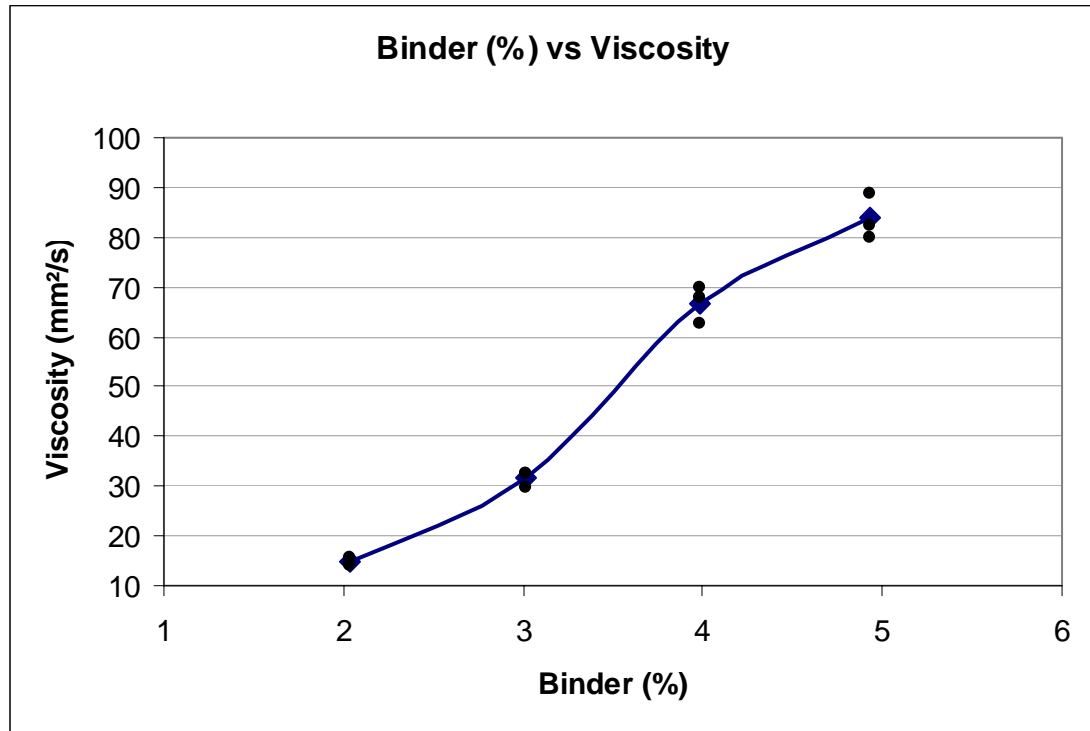


Figure 2: Plot of binder content vs viscosity

Drying Conditions

It was observed early on in the experiments that the drying rate of the TBC is dependent on temperature and humidity. Figure 2b shows the drying time as a function of ambient temperature and humidity. The drying rate is significantly improved if the ambient temperature is above 20°C and the humidity is approximately 28%.

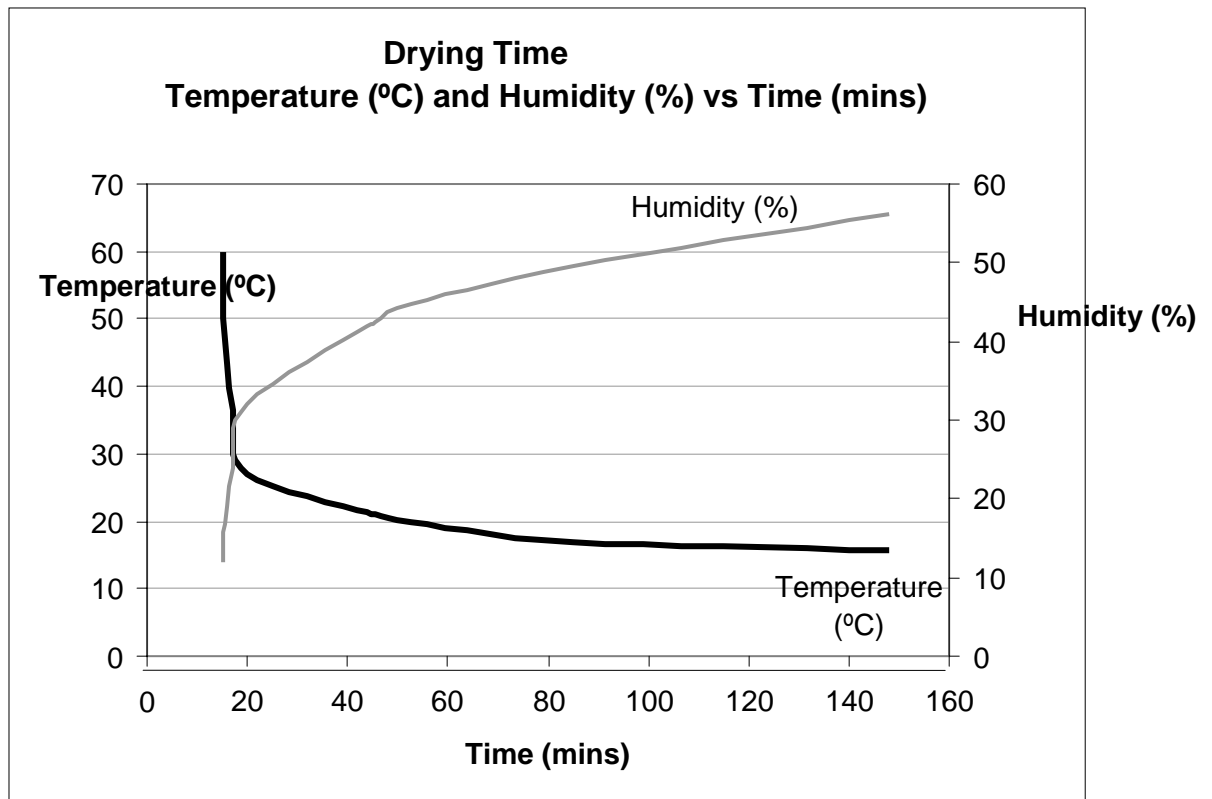


Figure 2b: Drying time of TBC as a function of temperature and humidity.

Pressure Stamping and Sintering

The optimum stamping pressure was found to be 20 MPa. This serves to reduce the sintering time needed to sinter the coating and hence, reducing the fabrication time. The optimum sintering time was found to be 20 – 40 minutes for both sintering in the oven and with an oxyacetylene torch mounted on an automated rig (Figure 3) to achieve consistent flame height. The oven sintering temperature was 800°C.

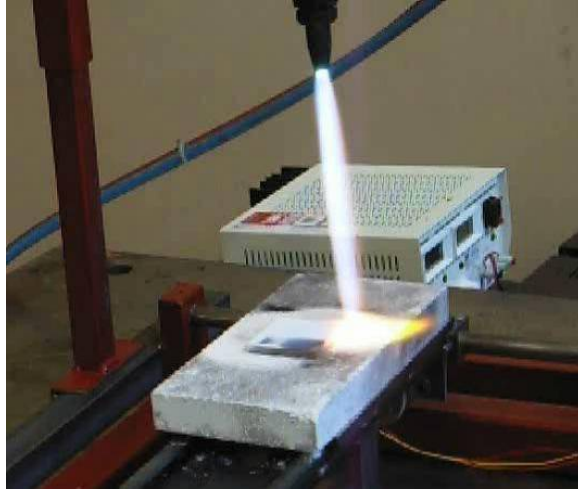


Figure 3: Automated Sintering Platform

The quality and durability of the fabricated coatings were assessed by microstructural analysis to examine the porosity, cracking and interfacial spallation. Adhesion tests were carried out with a PosiTest pull-off adhesion tester to measure the failure strength of the coatings. The coating-substrate specimens were exposed to thermal cycling consisting of 60 minutes of heating at 900°C and 30 minutes of cooling in a laboratory oven. Microstructural analysis and thermal / mechanical tests were conducted prior to and after each thermal cycle.

3. RESULTS AND VERIFICATION

3.1 MICROSTRUCTURAL ANALYSIS

Coating Thickness

The cross-sectional thickness of a 100% ceramic thermal barrier coating, estimated from the SEM of a spalled coating, is approximately 0.1mm. This is shown in Figure 4 below.

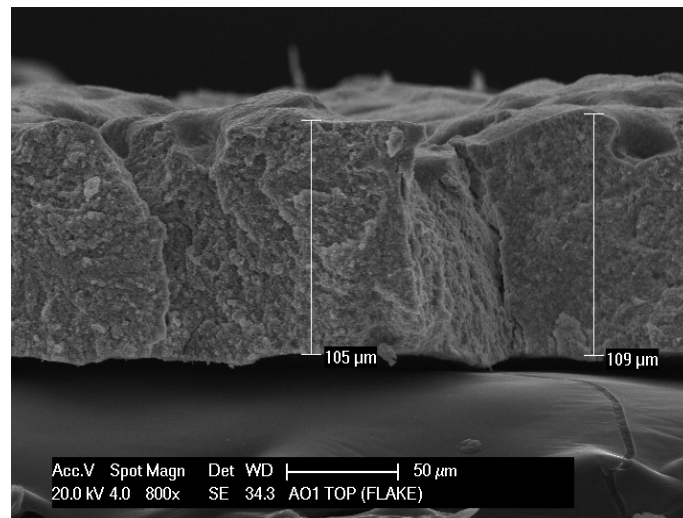


Figure 4: Approximate cross-sectional thickness of a single layer thermal barrier coating (100% ceramic).

Porosity Size

The cross sectional porosity embedded below the surface of the TBC is shown in Figure 5a. A plan view of the surface of the single layer (100% ceramic) TBC showing the porosity sizes is shown in Figure 5b.

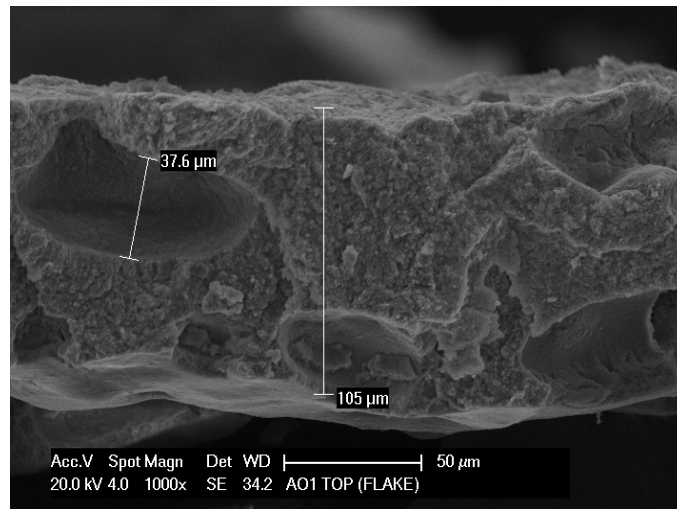


Figure 5a: Cross-sectional porosity measurement of a single layer (100% ceramic) TBC.

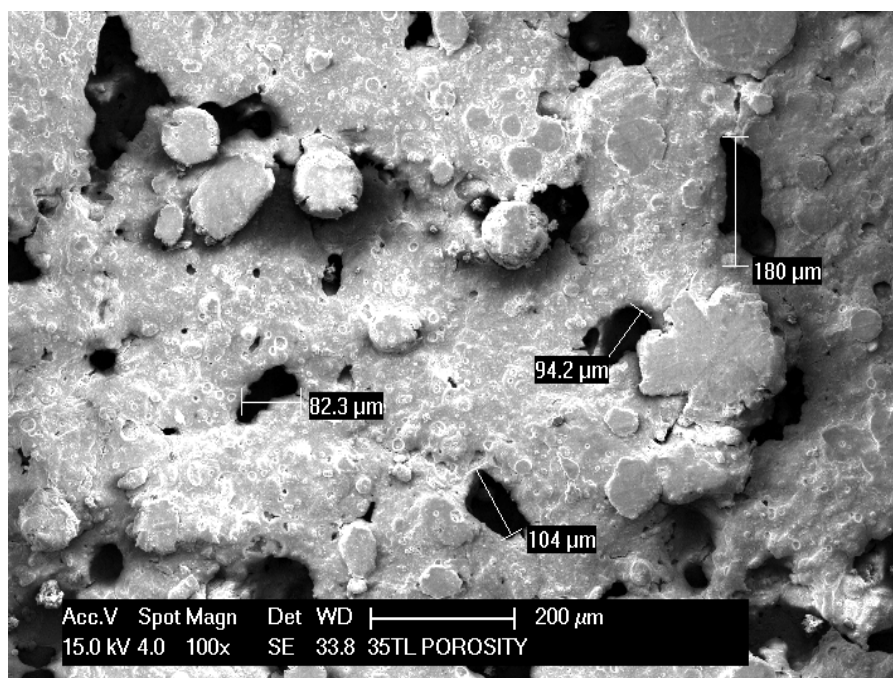
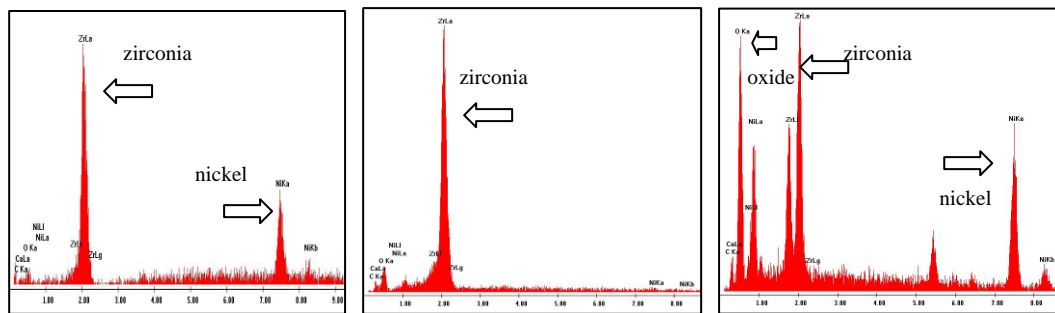
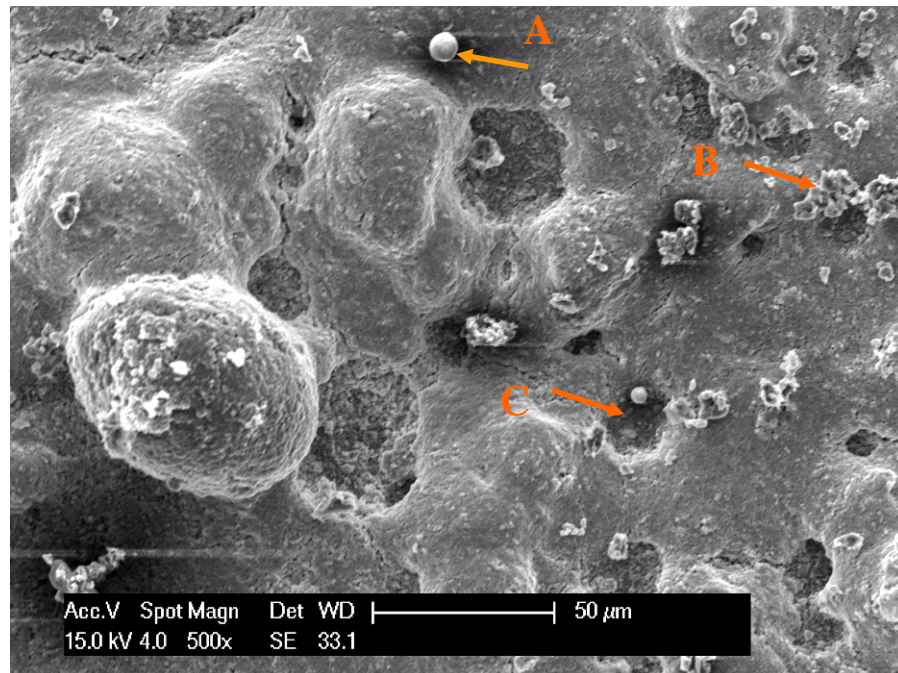


Figure 5b: Plan view showing porosity size measurement of a single layer (100% ceramic) TBC

Composition Analysis

The composition analysis of the TBC base layer (50% ceramic and 50% nickel) is shown in the Figure below. The actual percentage of nickel in the coating is slightly lower than that in the slurry mixture, suggesting some loss during the spraying process.



A

B

C

Figures 6a-d and 7a-d show the SEM of specimens of the 2-layer FGM TBC produced under different sintering conditions, as indicated in Table 2. The substrate was pure nickel (UNS N02200). For all the specimens, the base layer composition was 50% ceramic and 50% nickel and the top layer was 100% ceramic.

Specimen No.	Sintering conditions
1	Sintered for 20 mins with torch; 20 cm sintering height.
2	Oven sintered at 900°C followed by cooling at ambient temperature;
3	Sintered for 20 mins with torch; 15 cm sintering height
4	Oven sintered at 800°C followed by cooling at ambient temperature;

Table 2: Sintering conditions for different specimens of the 2 layer FGM TBC.

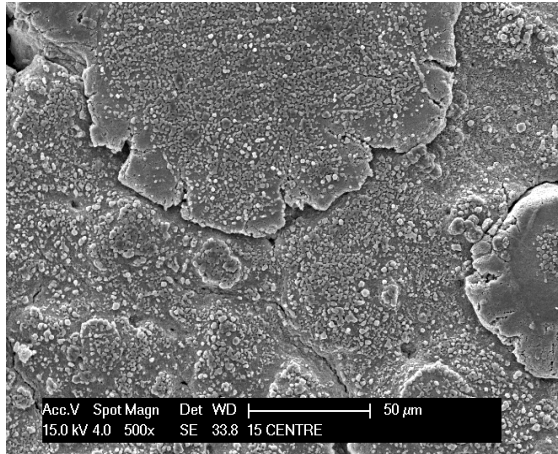


Figure 6a: Specimen 1, centre, 500x magnification.

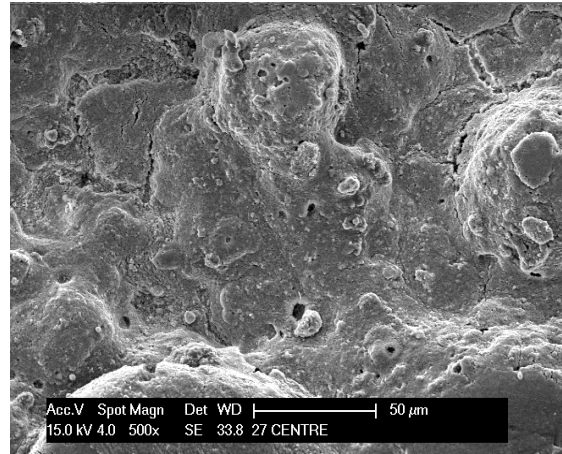


Figure 6b: Specimen 2, centre, 500x magnification.

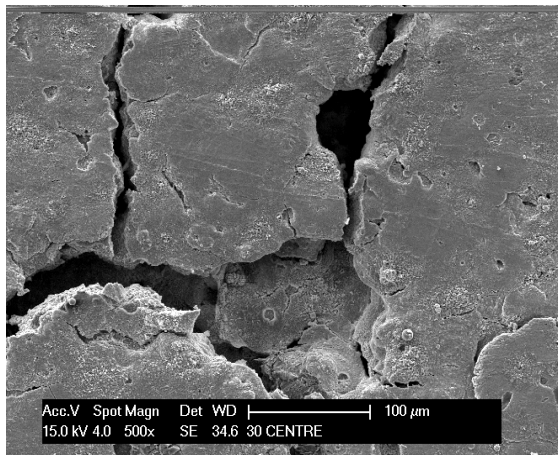


Figure 6c: Specimen 3, centre, 500x magnification.

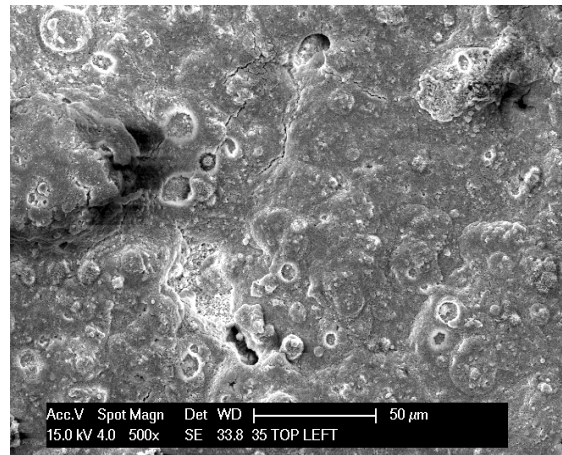


Figure 6d: Specimen 4, top left, 500x magnification.

From the SEM images, it can be seen that specimen 1 (torch sintered for 20 minutes) had small granular microstructure spreading across the surface. Specimen 2 (sintered in oven at 900°C and cooled slowly at ambient temperature) had a higher surface roughness where the differences in heights were apparent with the smooth profile. Specimen 3 (torch sintered at a lower height compared to specimen 1) had a very smooth and flat surface area with visible porosity and cracks. Specimen 4 (sintered in oven at 800°C followed by cooling at ambient temperature) had small circular patterns across the surface area.

Porosity Observation

Overall Top View

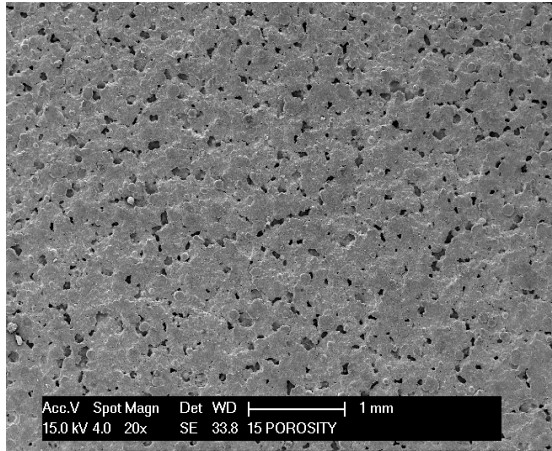


Figure 7a: Specimen 1, centre, 20x magnification.

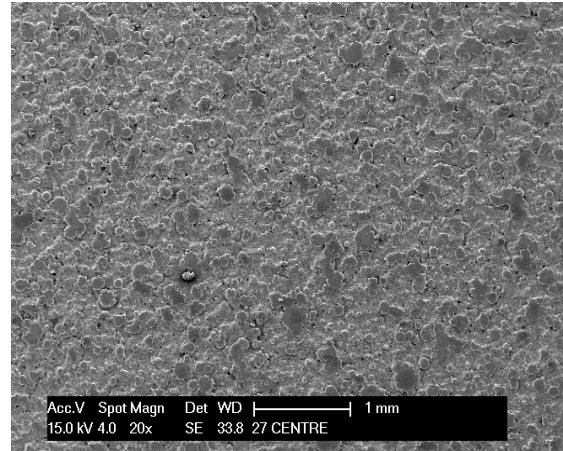


Figure 7b: Specimen 2, centre, 20x magnification.

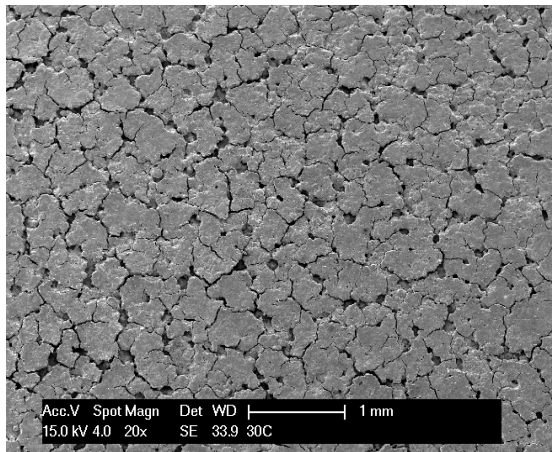


Figure 7c: Specimen 3, centre, 20x magnification.

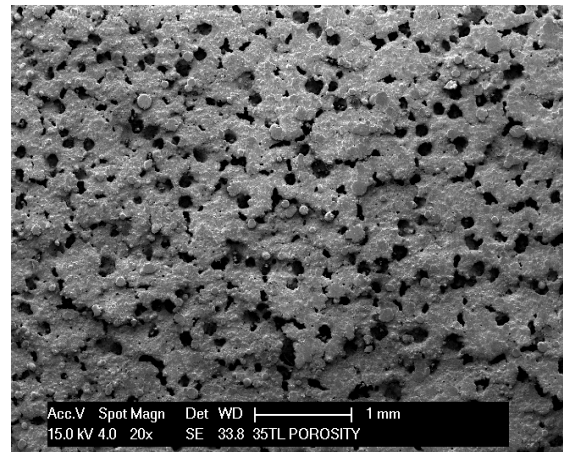


Figure 7d: Specimen 4, top left, 20x magnification (centre spalled).

From the SEM images in Figures 7a-d the porosity can be compared for each specimen prepared under the different sintering conditions as listed in Table 2. Variations in porosity size, crack size and propagation can be observed. It can be seen that specimen 2 had the lowest visible porosity followed by specimen 1 and 3. Specimen 4 is the most porous. The amount of porosity on specimen 2 was the most desirable.

Porosity Size Approximation

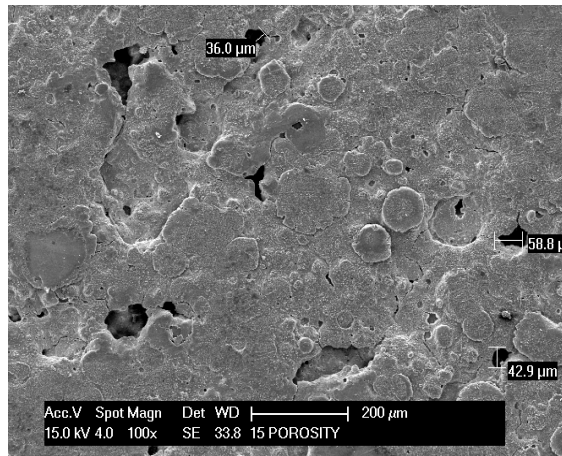


Figure 8a: Specimen 1, centre, 100x magnification.

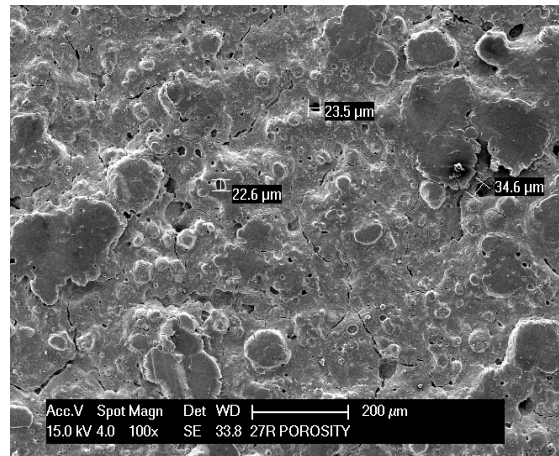


Figure 8b: Specimen 2, right, 100x magnification.

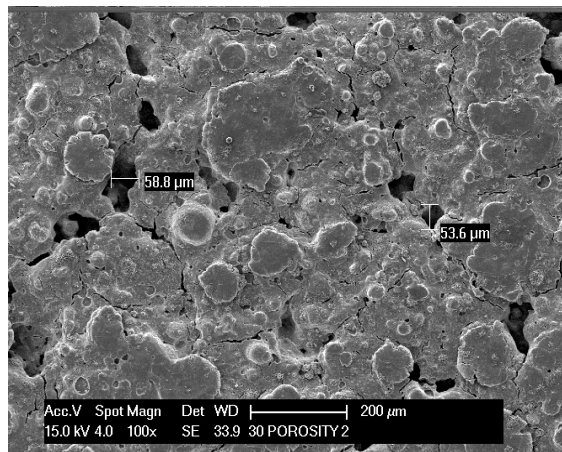


Figure 8c: Specimen 3, centre, 100x magnification.

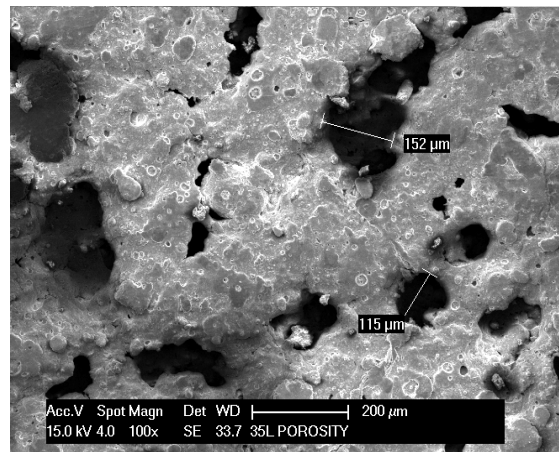


Figure 8d: Specimen 4, left, 100x magnification.

Figures 8a-d show the estimated porosity sizes on the SEM images under a higher magnification for the specimens prepared under the different sintering conditions. They are consistent with the conclusions drawn from visual observation of the coatings and the SEM images shown in Figures 7a-d.

Porosity Improvements

The surface porosity of the 2 layer functionally graded TBC is shown in Figure 9 below:

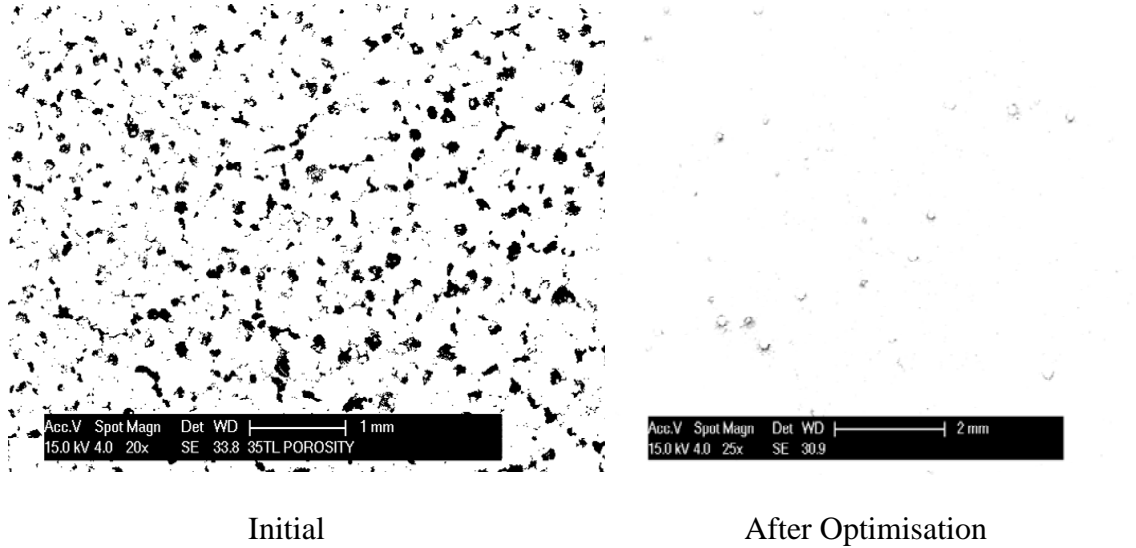


Figure 9: Scanning Electron Microscope (SEM) images of TBC before and after optimisation of mixing and spraying technique.

Through improvements of the fabrication techniques as mentioned in the previous section, the surface porosity had been effectively reduced from 15% to 0.5% in accordance with ASTM E2109-01. Hence, a 97% reduction in surface porosity had been achieved.

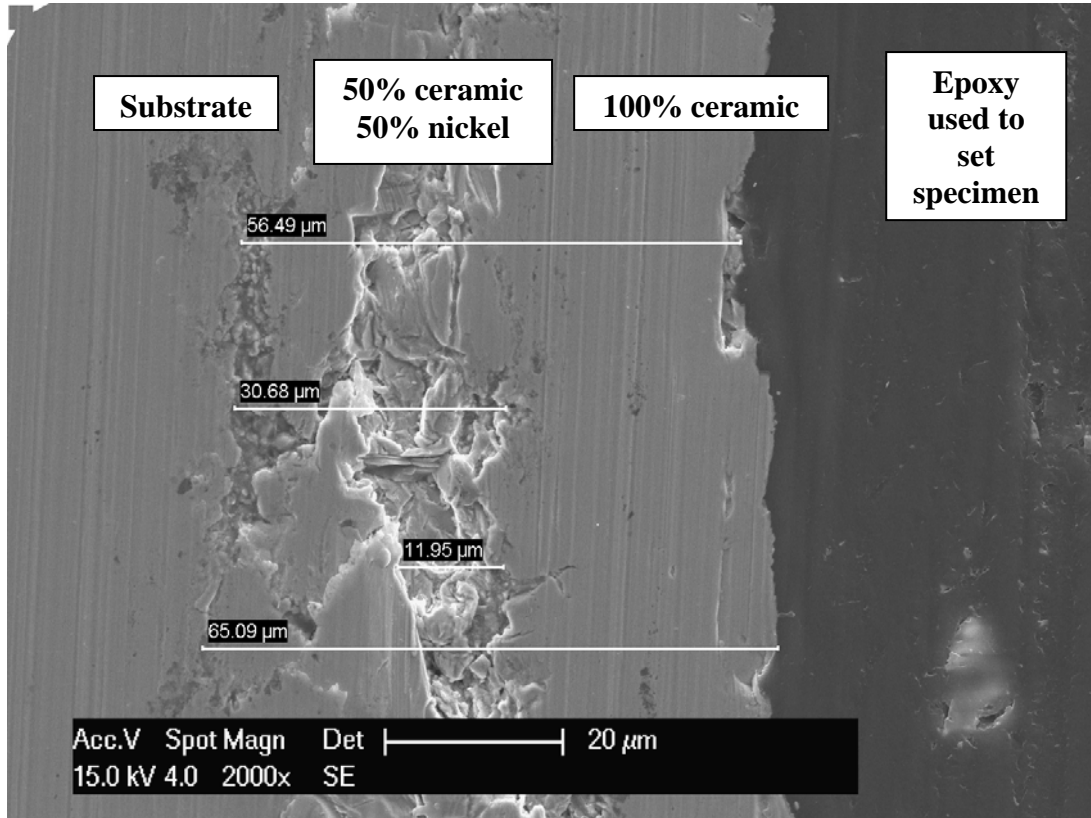


Figure 10a: Porosity distribution around the cross-sectional area of the FG TBC.

Figure 10a shows the SEM image of the porosity distribution around the cross-sectional area of the FG thermal barrier coating. The porosity distribution of the FGM TBC follows closely with the theoretical hypothetical graded structure illustrated by Miyamoto et. al.³³ (see Figure 10b). Through stamping, the loosely packed surface layers on the right of Figure 10a, consisting of small particle size were compacted and porosities located in the mid section were filled, hence leaving small porosities trapped between the larger particles densely located near to the surface of the substrate. A comparison of the percentage of porosity in the various TBC coatings is shown in Figure 11. The porosity of the 2-layer FGM TBC is around 0.5%, slightly higher than the 100% ceramic coating.

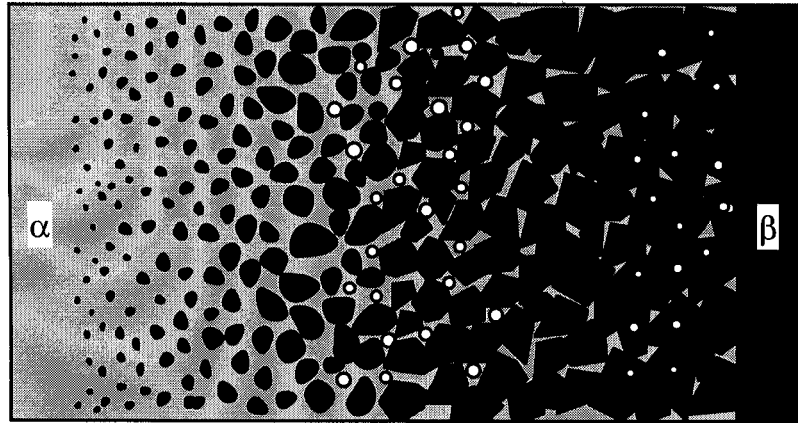


Figure 10b: Diagram of a hypothetical graded structure that has gradients in several different microstructural features (Miyamoto, et. al., Reference [33]).

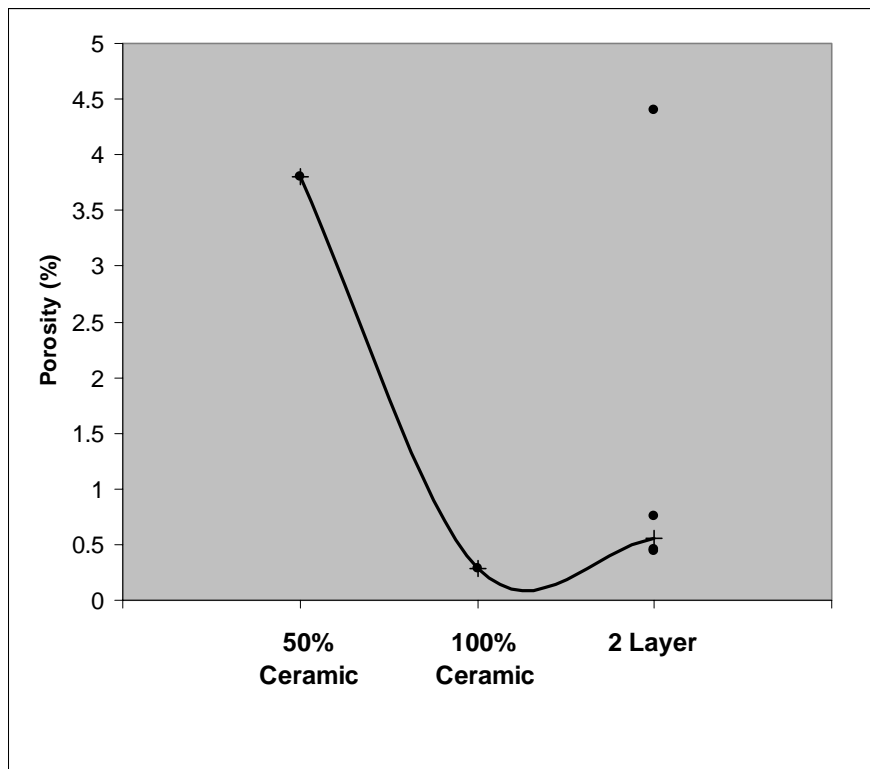


Figure 11: Comparison of Percentage of Porosity in the TBC coatings

3.2 Thermal and Mechanical Testing

3.2.1 Thermal Cycling

To compare the effectiveness and durability of the different TBC coatings, the specimens were exposed to up to 22 thermal cycles, each cycle consisted of 60 minutes at 900°C followed by 30 minutes of cooling. The following coating-substrate systems were tested:


Coating-Substrate (Ni) System	No. of specimens tested
100% ceramic	3
50% ceramic / 50% nickel	6
2-layer FGM TBC as illustrated below: 	6

Figure 12 shows the number of specimens surviving the thermal cycling tests. Failure occurs when there are visible signs of spallation in the TBC specimen after a thermal cycle. The failed specimens were removed from the oven for microstructural analysis. The results show that the majority of failure occurred early on during the first or fourth cycle. Specimens that survived the fourth cycle remained in good condition.

The number of failure resulting from thermal cycling of specimens prepared under different sintering conditions was also compared (see Figure 13). The results showed that the oven sintered 2-layer FGM TBC performed best after 22 thermal cycles. This observation is consistent with results reported in the literature which suggests that TBCs manufactured under controlled sintering and cooling environments performed better in real life applications. By applying a constant heat flow, uniform heat expansion and ideal boundary grain growth between particles can be achieved, thus reducing thermal stress induced during the thermal expansion process. Also, a slow cooling rate after sintering effectively reduces the strain and

stress associated with rapid cooling. As expected, introduction of a functionally graded coating produced better performance compared to a single layer of ceramic TBC as the FGM reduces the thermal gradient across the specimen and hence, minimises the thermal mismatch due to cooling and the resulting residual stresses.

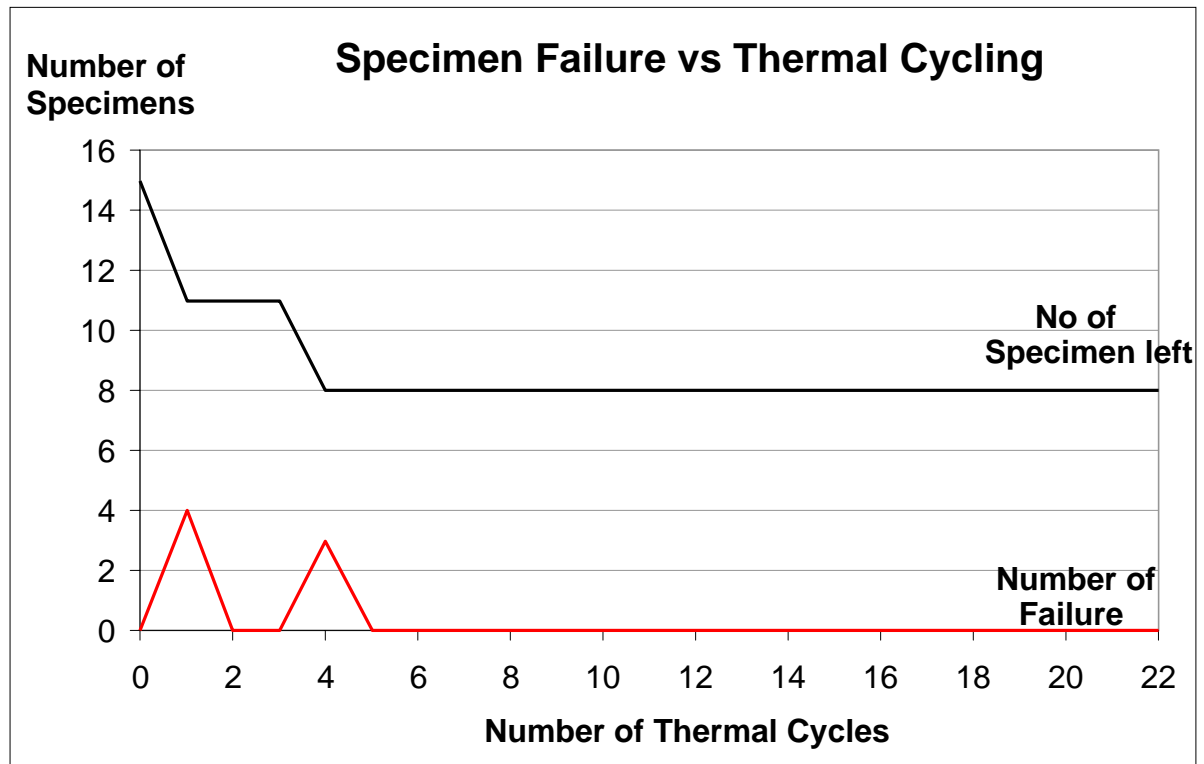


Figure 12: Plot of number of specimens failure vs number of thermal cycles

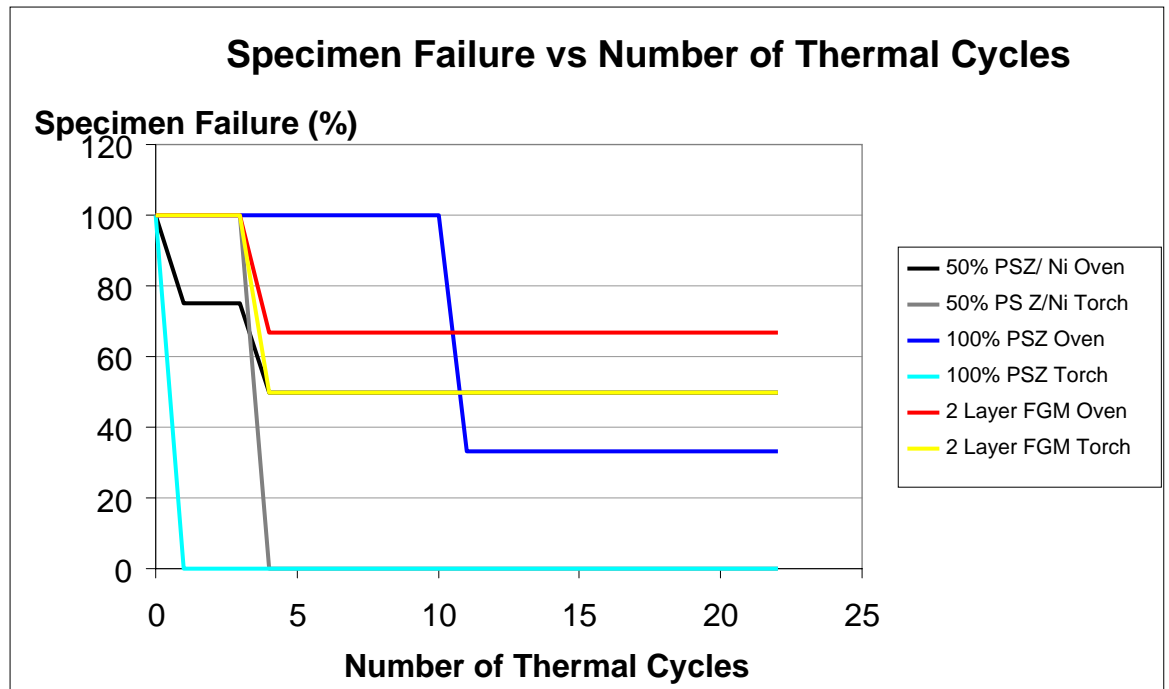


Figure 13: Plot of number of specimens failure vs number of thermal cycles

Figure 14 shows the SEM image of a specimen that has survived 10 thermal cycles. The SEM images of the TBC specimens that have failed during thermal cycling are shown in Figures 15 a-c. They show that the individual porosities in the specimen before thermal cycling evolved into fine cracks inter-linking the porosities after 10 thermal cycles. After 20 thermal cycles, the cracks and porosities increased in size.

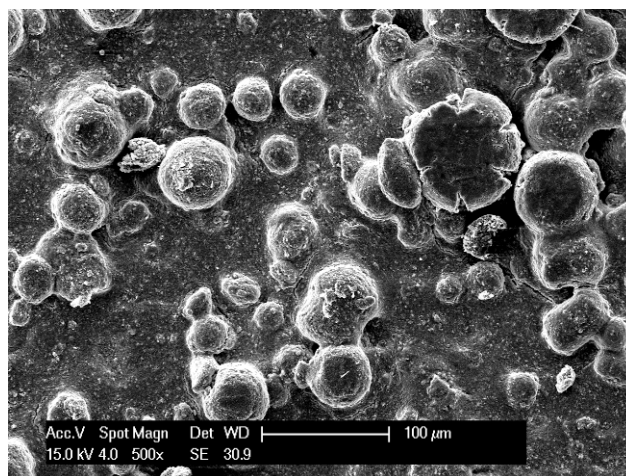


Figure 14: Microstructure of a torch sintered 2-layer FGM TBC after surviving 10 thermal cycles.

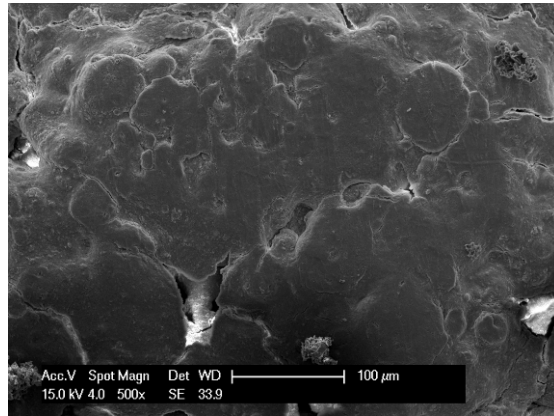


Figure 15a: Before thermal cycling.

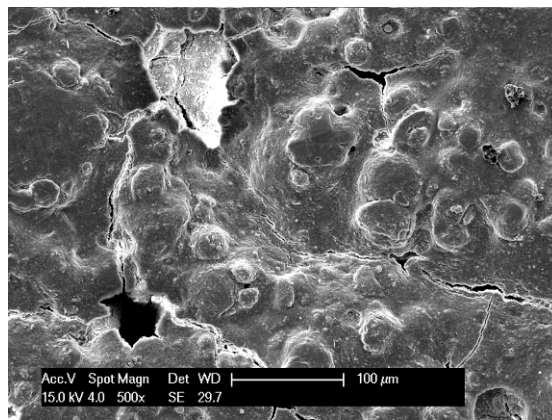


Figure 15b: After 10 thermal cycles.

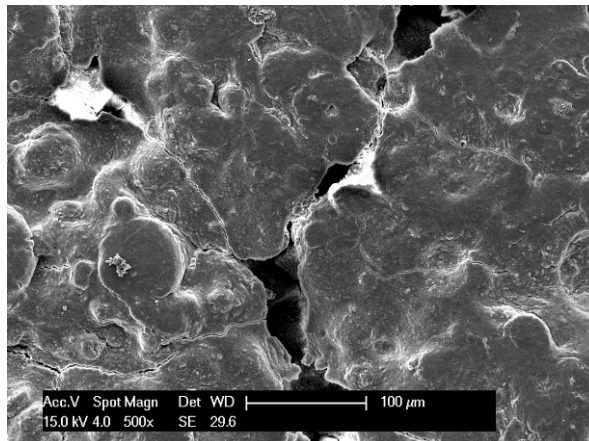


Figure15c: After 20 thermal cycles.

Figure 15 a-c: Microstructure of oven sintered 2-layer FGB TBC before and after thermal cycling.

3.2.2 Adhesion test

The adhesion of the TBC layer is one of the most important parameter that determines the durability of the TBC system as the spallation / delamination of the coating has a crucial influence on its function and life expectancy. A PosiTest pull-off tester (designed to meet ASTM D4541 and D7234 standard) was used to perform the adhesion tests (see Figure 16). The accuracy of this tester is $\pm 1\%$.



Figure 16: PosiTest pull-off adhesion tester (DeFelsko Corporation, 2008)

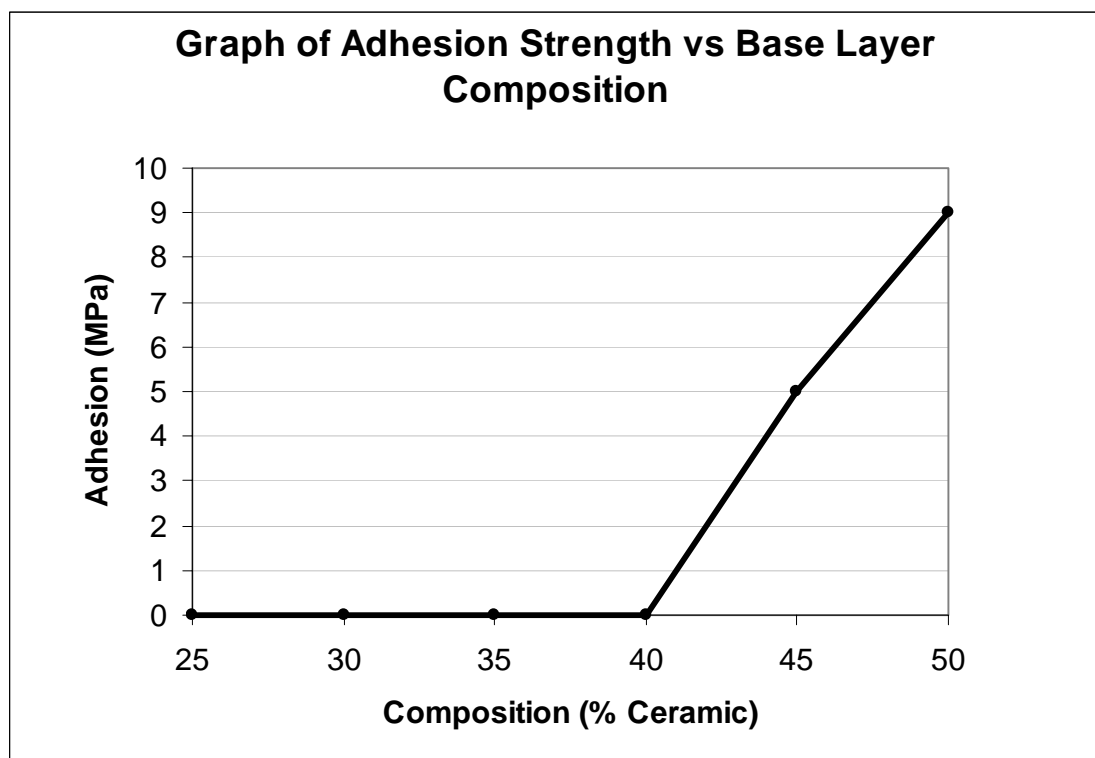


Figure 17: Plot of TBC composition vs Adhesion strength.

The adhesion strengths of single layer TBCs consisting of zirconia and nickel ranging in composition from 25% to 50% zirconia are shown in Figure 17. For the TBCs with composition of less than 40% zirconia, spalling occurred almost immediately after the sintering process, during cooling at ambient temperature. The adhesion strength increases almost linearly at a rate of 0.9 MPa per 1% increment of zirconia in the composition and peaks at a 50/50 ceramic / nickel composition with adhesion strength of 9 MPa. However, further improvement in the properties of the base layer is restricted by constraints such as residual stress caused by the mismatch in thermal expansion coefficients of the substrate to the zirconia coating. Moreover, if the content of the slurry mixture exceeds 50% zirconia, flocculated slurry was produced, introducing surface irregularities during spraying which will induce problems such as uneven pressure application during pressure stamping and eventually generating cracks and spalling after the sintering process.

The results from the adhesion tests of various TBCs with a single layer (100% ceramic, or 50% ceramic and 50% nickel) and two layers (functionally graded) are shown in Figure 18. They clearly show the almost 100% improvement in adhesion strength of the functionally graded (2 layers) TBC compared to the 100% ceramic TBC and 25% improvement in adhesion strength compared to the 50% ceramic TBC. The maximum adhesion strength obtained for the 2-layer FGM TBC was 11 MPa. Although this is lower than the adhesion strength produced by more expensive techniques (such as plasma spraying, flame spray method), further improvement in adhesion strength may be achieved by adding another FG layer to the TBC or by adding a bond coat to the substrate prior to the base layer. It should also be noted that the adhesion strength of this 2-layer FGM TBC may be sufficient for applications such as expendable hypersonic vehicles which do not require the TBC to have a long life expectancy. For such applications, the slurry spray and sintering technique is relatively simple and cost effective and hence, has considerable advantages over the more expensive techniques.

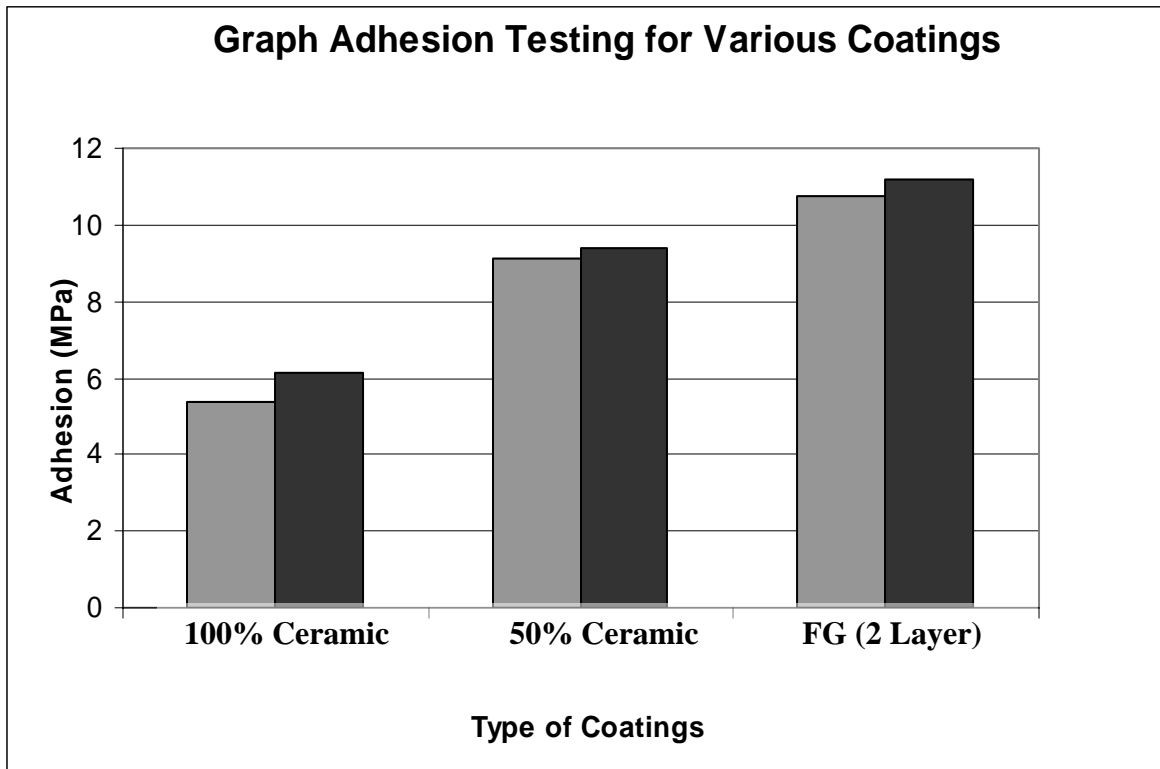


Figure 18: Graph of adhesion testing for various TBCs.

6. Summary and Future Plans

An earlier study supported by the AOARD under contract number AOARD-064043, conducted a feasibility study of a relatively simple and economical method for producing functionally graded thermal barrier coatings using the Wet Powder (Slurry) and Sintering method. This method is relatively undeveloped and under utilised compared to more expensive techniques such as chemical vapour deposition, physical vapour deposition, plasma spraying and powder metallurgy. It utilises a pressurised spray gun to spray a slurry mixture of the powdered coating material suspended in a liquid solution directly onto a substrate surface followed by sintering using an oxyacetylene torch.

The effects of slurry composition, type of ceramic powder, compatibility with substrates, spraying and sintering conditions were studied. Several TBC specimens have been fabricated under various conditions to develop a procedure which produce good quality coatings (of up to 3 layers) with little or no spallation. The optimum time, heat flux and applied pressure level for sintering were deduced. TBCs produced from a 40-45% ceramic, 4% binder and 0.4% dispersant composition and sintered for 30 minutes with an applied pressure of 30 MPa produced good quality coatings with a uniform and very smooth surface. Scanning electron micrographs of the fabricated TBC coatings showed good contact between the grain boundaries of the ceramic powder.

In the current project (AOARD 084003), the Wet Powder and Sintering method is further developed. Improvements to this method include automating the sintering procedure and optimising the fabrication conditions. A much more extensive microstructural and thermal and mechanical testing program is conducted to obtain a more qualitative measure of the quality and durability of the FGM thermal barrier coatings and to develop high temperature constitutive models for input into the finite element thermal-structural modelling of FGM structures.

The mean-field micromechanical approach was applied to design ceramic-metal FGM thermal coatings (see reference 32). This analysis took into consideration the microscopic inelastic deformation in each constituent phase such as plastic and

creep, as well as the diffusional mass flow at the interface between ceramic and metal phases. Through the investigation of a case study for Ni-ZrO₂ FGM TBCs, the fundamental strategy to seek for optimal ceramic-metal FGMs was proposed. From the viewpoints of overall heat-transfer coefficient and average density of the FGM, it is better that the gradation parameter is larger, which means average volume fraction of ceramic phase is larger. Therefore, based on this strategy, it is conducted to set the gradation parameter larger within the range that thermal fracture does not occur. For various mechanical boundary conditions, the most suitable compositional parameters were decided. Creep of ceramics near the ceramic surface has a big influence on the thermal stress states in FGMs, which can cause extremely large tensile stress during the cooling process. In order to prevent thermal stress-induced fracture due to creep of ceramics, creep of ZrO₂, which can be a cause of thermal fracture, should be avoided. Extensive experimental work is needed to validate the numerical results obtained in our earlier study and this is planned for the next phase of this study (Option 1).

An analytical method, developed in an earlier study^{7,8} by one of the authors, to predict the aero-thermal and structural response of hypersonic vehicles was used to determine the design criteria, such as temperature limits, for the FGM thermal barrier coating. This analysis tool will assist the design of FGM coatings at the material and global levels. At the material level, the micromechanics models described in our earlier study are implemented in the finite element (FE) thermal-structural models of the FGM TBCs to determine the number of layers required to protect the metal structure (substrate), for example the leading edge and combustor, from the aerodynamic and combustion heating loads seen in hypersonic flights. This is the subject of further study.

In the follow-on study (Option 1), the thermal and mechanical properties of the FGM TBC will be studied in more details to develop constitutive models for the various FGM layers with different PSZ/Ni compositions, to provide the input data for FE thermal-structural analysis. A more detailed thermal and mechanical testing program will be conducted on the FGM TBCs prior to and after thermal cycling. These tests will include thermal conductivity, micro-hardness indentation tests, adhesion tests and instron tensile tests at elevated temperatures.

5. Acknowledgements

The authors would like to thank Dr J.P. Singh and Dr Kumar Jata of AOARD for their helpful discussions and support.

The authors acknowledge the contributions of Syed Abdul Khaliq Syed Ihsan, Ho Chyi Perng and Tan Kin Keam in fabricating the thermal barrier coatings and conducting the experiments as part of their final year mechanical engineering project.

6. References

1. K. Wakashima and H. Tsukamoto, *Proc. of the 1st Int. Symp. on Functionally Gradient Materials*, FGM Forum, (1990), pp.19-26
2. K. Wakashima, H. Tsukamoto and T. Ishizuka; *Proc. of the 13th Risø Int. Symp. on Metall. Mater. Sci.*, Risø National Laboratory, (1992), pp.503-510.
3. H. Tsukamoto, A. Kotousov, S.Y. Ho, J. Codrington, *Proceedings of the Structural Integrity and Failure Symposium*, (2006) pp. 25
4. K. Wakashima and H. Tsukamoto: *Proc. of the 1st Int. Symp. on Functionally Gradient Materials*, FGM Forum, (1990), pp.19-26.
5. K. Wakashima, H. Tsukamoto and T. Ishizuka; *Proc. of the 13th Risø Int. Symp. on Metall. Mater. Sci.*, Risø National Laboratory, (1992), pp.503-510.
6. H. Tsukamoto and A. Kotousov, *Key Engineering Materials*, Vols. 340-341 (2007) pp. 95-100
7. S.Y. Ho and A. Paull, *Aerospace Science and Technology*, 10 (2006) pp. 420-426
8. S.Y. Ho, *Proceedings of the 14th AIAA.AHI Space Planes and Hypersonic Systems and Technologies Conference*, AIAA-2006-8070, (2006).
9. S. Harding, *Final Year Project Preliminary Report*, University of Adelaide (2007)
10. DC Callister, *Fundamentals of Materials Science and Engineering*, 5th edn, 2003, Wiley, NY.
11. M Fevre, A Finel & R Caudron , ‘Local order and thermal conductivity in yttria-stabilized zirconia’, *Laboratoire d’Etude des Microstructures*, Onera, Chatillion, France, 2004.

12. A Ruder, HP Buchkremer, H Jansen, W Mallener & D Stover, 'Wet powder spraying – A process for the production of coatings', *Surface and Coatings Technology Journal*, 1992, vol. 53, pp. 7174.
13. E.P Degarmo, JT Black & RA Kohser, *Materials and Processes in Manufacturing*, 9th edn, 2003, Wiley International, USA
14. P Roy, G Bertrand & C Coddet, 'Spray drying and sintering of zirconia based hollow powders', *Powder Technology Journal*, 2005, vol. 157, pp. 20-26.
15. Mills, AF 1999, *Heat Transfer*, 2nd edn, PrenticeHall, Sydney
16. A. E. Giannakopoulos, S. Suresh, M. Finot and M. Olsson: *Acta Metallurgica et Materialia*, 1995, vol. 43 (4), pp. 1335-1354.
17. M. -J. Pindera and P. Dunn: *Composites Part B: Engineering*, 1997, vol. 28(1-2), pp. 109-119.
18. M. Grujicic and Y. Zhang: *Materials Science and Engineering A*, 1998, vol. 251 (1-2), pp. 64-76.
19. J. Aboudi, M. -J. Pindera and S. M. Arnold: *Composites Part B: Engineering*, 1999, vol. 30 (8), pp. 777-832.
20. J. D. Eshelby: *Proc. R. Soc. London*, 1957, A241, pp. 376-396.
21. J. D. Eshelby: *Proc. R. Soc. London*, 1959, A252, pp. 561-569.
22. J. D. Eshelby: *Prog. Solid Mech.*, 1961, vol. 2, pp. 89-140.
23. M. Taya, J. K. Lee and T. Mori: *Acta Materialia*, 1997, vol. 45 (6), pp. 2349-2356.
24. K. Tohgo, A. Masunari and M. Yoshida: *Composites Part A*, 2005, in Press.
25. H. Tsukamoto: *Composites Part B*, 2003, vol. 34 (6), pp. 561-568.
26. T. Mori, M. Okabe and T. Mura, *Acta Metall.*, 1979, vol. 28, pp.319-325.
27. M. Z. Berbon and T. G. Langdon, *Acta Mater.*, 1998, vol. 46, pp.2485-2495.
28. N. G. Pace, G. A. Saunders, Z. Stimengen, and J. S. Thorp: *J. Mater. Sci.*, 1969, vol. 4, pp. 1106-1110.
29. H. J. Frost and M. F. Ashby: *Deformation Mechanism Maps*, Pergamon Press, Oxford, 1982.
30. A. Kawasaki and R. Watanabe: *Engineering Fracture Mechanics*, 2002, vol. 69 (14-16), pp.1713-1728.

31. J. Codrington, P. Nguyen, S.Y. Ho and A. Kotousov, *Applied Thermal Engineering Journal*, submitted May 2007.
32. S.Y. Ho, A. Kotousov, P. Nguyen, S. Harding, J. Codrington and H. Tsukamoto, *FGM (Functionally Graded Material) Thermal Barrier Coatings for Hypersonic Structures – Design and Thermal Structural Analysis*
AOARD-064043 FINAL REPORT
33. Y. Miyamoto, W.A. Kaysser, B.H. Rabin, A. Kawasaki, R.G. Ford:
Functionally Graded Materials: Design, Processing and Applications, Kluwer Academic Publishers, London 1999.